ENCIT 2018

ABCM Associação Brasileira de Engenharia e Ciências Mecânicas

17th Brazilian Congress of Thermal Sciences and Engineering
November 25th-28th, 2018, Águas de Lindóia, SP, Brazil

ENCIT-2018-0017
EFFECT OF THE MACRO-SCALE TOPOLOGY OVER THE EFFECTIVE DRAG COEFFICIENT IN DENSE GAS-SOLID FLUIDIZED FLOWS

Seyed Reza Amini Niaki
Joseph Mouallem
Christian C. Milioli
Fernando E. Milioli
Department of Mechanical Engineering, School of Engineering of Sao Carlos, University of Sao Paulo, 13566-590 Sao Carlos SP, Brazil
r.amini@usp.be; josephmouallem@usp.br; ccosta@sc.usp.br; milioli@sc.usp.br

Abstract. *Large scale simulation of fluidized gas-particle flows with two-fluid modeling requires closure models to deal with sub-grid filtered parameters such as filtered and residual stresses and filtered drag. The very heterogeneous topology of the concerning flows is qualitatively well captured by the current two-fluid formulations, but quantitative accuracy is still out of reach mostly due to the lack of more accurate sub-grid closure models. The effective drag coefficient is one of those closures for which sub-grid modeling requires improvement. Literature presents models for the effective drag coefficient derived from results of highly resolved simulations with two-fluid modeling which disregard any macro-scale impact. In this work it is showed that macro-scale effects cannot be disregarded if higher accuracy is pursued. The macro-scale parameters considered were the domain average solid volume fraction and gas flow Reynolds number, both showing significant effects over the effective drag coefficient. Only dense gas-solid flows were considered, as a complement to a previous work dealing with dilute conditions (Niaki et al., "Effect of the flow Macro-Scale on the effective drag coefficient in Gas-Solid flows", COBEM2017).*

Keywords: *Gas-solid flow, Macro-scale, Dense fluidized bed, Effective drag*

1. INTRODUCTION

This investigation deals with the problem of accurately predicting gas-particle flows in dense fluidized beds through two-fluid modeling, where gas and particulate are both treated as interpenetrating continuum phases (Anderson and Jackson 1967, Igci and Sundaresan 2011, Gidaspow 1994, Enwald et al. 1996). Two-fluid formulations, which are widely applied in large-scale simulation of gas-particle fluidized flows, require closure models to recover sub-grid information that are filtered by the coarse meshes that are usually applied. Among the parameters requiring sub-grid closuring are filtered and residual stresses on both phases and interphase interactions, mostly effective drag. This work is intended to analyze the behavior of the effective drag coefficient for dense gas-particle fluidized flows as a contribution to future developments of new improved formulations of sub-grid drag models.

A line of development of sub-grid models is followed which is based on filtering over results of highly resolved simulations with microscopic two-fluid modeling. This procedure has been widely practiced in literature (Agrawal et al. 2013, Andrews IV et al. 2005, Igci and Sundaresan 2011, Parmentier et al. 2012, Ozel et al. 2013, Milioli et al. 2013, Schneiderbauer and Pirker 2014, Sarkar et al. 2016), providing sub-grid models that, nevertheless, require continuing improvement in order to remove shortcomings and drawbacks. The sub-grid models are also called meso-scale models since they are generated from computational experiments under grid refinements that are expected to capture all the solid phase scales of the flow, so that filtered meso-scale data can be derived. In most cases, reduced domains are considered, which are extracted from the free stream in the core of the flow field, and periodic boundaries are applied. As periodic boundaries are applied, an extra gas phase pressure gradient is imposed in the vertical direction in order to impose a flow driving force. It is usual to consider an extra gas phase pressure gradient to exactly compensate the gravity acting on the gas-solid mixture.

The usual literature approach gives rise to low velocity suspensions which are assumed to prevail at the sub-grid level of any flow topology, from very dilute to very dense. This assumption is consistent with the scale separation hypothesis, which nevertheless is quite questionable in view of the lack of scale separation that prevails in gas-solid fluidized flows (van der Hoef et al., 1997). The usual approach is questioned in the current work, where an investigation is advanced on the effect of topology related effects over the sub-grid data, specially related to the effective drag coefficient under dense flow conditions of concern. This is done by developing new highly resolved simulations in periodic domains, under imposed domain average solid volume fractions at dense conditions, and domain average gas Reynolds numbers from those for very low suspensions up to those for conditions approaching pneumatic transport. Results show that both the macro-scale imposed parameters considerably affect the effective drag coefficient, and should therefore be accounted for if higher accuracy is pursued.

2. Methodology

2.1 Microscopic two-fluid model

To probe the behavior of the flow at Meso-scale structures, the numerical integration of the two-fluid model conservative equations was proposed with the postulate of a fixed control volume for both phases (Anderson and Jackson 1967, Mouallem et al. 2018). Integral balances can be applied to the mass, momentum, and energy equations. Meantime, by utilizing Gauss and Leibniz theorems, the integral balances are converted into instantaneous differential equations and jump conditions. Eventually, averaging operators are applied so that the continuum hypothesis holds for the interpenetrating phases. In this model, kinetic theory of granular flows is employed to the solid phase, which includes an equation for granular energy conservation (Lun et al. 1984, Gidaspow 1994). This equation provides a granular temperature to which continuum properties for particulate phases are correlated. Also, the gas-solid interface interaction is frequently described as a drag effect of the gas over the solid phase, usually through empirical correlations such as that of Wen and Yu (1966). The microscopic two-fluid model is here partially presented in Tab. 1, emphasizing the closures of main interest in the present work.

Table 1. Microscopic two – fluid model

Conservation equations of continuity and momentum for both phases

1) $$\frac{\partial\left(\rho_s\phi_s\right)}{\partial t}+\nabla.\left(\rho_s\phi_s\mathbf{v}_s\right)=0$$

2) $$\frac{\partial\left(\rho_g\phi_g\right)}{\partial t}+\nabla.\left(\rho_g\phi_g\mathbf{v}_g\right)=0$$

3) $$\left[\frac{\partial\left(\rho_s\phi_s\mathbf{v}_s\right)}{\partial t}+\nabla.\left(\rho_s\phi_s\mathbf{v}_s\mathbf{v}_s\right)\right]=-\nabla.\boldsymbol{\sigma}_s-\phi_s\nabla.\boldsymbol{\sigma}_g+\boldsymbol{M}_I+\rho_s\phi_s\mathbf{g}$$

4) $$\left[\frac{\partial\left(\rho_g\phi_g\mathbf{v}_g\right)}{\partial t}+\nabla.\left(\rho_g\phi_g\mathbf{v}_g\mathbf{v}_g\right)\right]=-\phi_g\nabla.\boldsymbol{\sigma}_g-\boldsymbol{M}_I+\rho_g\phi_g\mathbf{g}$$

Volumetric continuity

5) $$\phi_s+\phi_g=1$$

Conservation equation of granular (or pseudo-thermal) energy

6) $$\left[\frac{\partial\left(\frac{3}{2}\rho_s\phi_sT\right)}{\partial t}+\nabla.\left(\frac{3}{2}\rho_s\phi_sT\,\mathbf{v}_s\right)\right]=-\nabla.\mathbf{q}-\boldsymbol{\sigma}_s:\nabla\mathbf{v}_s+\Gamma_{\text{slip}}-J_{\text{coll}}-J_{\text{vis}}$$

Closure for drag

7) $$\boldsymbol{M}_I=\beta\left(\boldsymbol{v}_g-\boldsymbol{v}_s\right)$$

8) $$\beta = \frac{3}{4} \mathrm{C_D} \frac{\rho_g \phi_g \phi_s \left| \mathbf{v}_g - \mathbf{v}_s \right|}{d_p e_p} \left(\phi_g \right)^{-2.65} \quad \text{Wen \& Yu (1966)}$$

9) $$\mathrm{C_D} = \begin{cases} \frac{24}{\mathrm{Re}_g} \left(1 + 0.15 \mathrm{Re}_g^{0.687} \right) & \mathrm{Re}_g < 1000 \\ 0.44 & \mathrm{Re}_g \geq 1000 \end{cases} \quad ; \quad \mathrm{Re}_g = \frac{\phi_g \rho_g d \left| \mathbf{v}_g - \mathbf{v}_s \right|}{\mu_g}$$

Further closures may be found in Mouallem et al. (2018).

2.2 Filtered two-fluid model

This article shows the behavior of a filtered effective drag in dense gas-solid flow which is required as sub-grid closure in large-scale simulations using two-fluid filtered formulations. Meantime, Filtered formulation for accounting the effective drag is shown in Table. 2. This formulation is achieved by applying a volumetric filter over the microscopic model equations given in Table. 1. Additionally, filtering procedure introduces new terms into the momentum equations in addition to those of the microscopic formulation. One such a term accounts for fluctuations on the buoyancy force exerted by the gas over the solid phase. This interface force is frequently added to the filtered drag force, defining an effective force usually referred to as effective drag owing to drag's predominance in gas-solid fluidized flows.

Table 2. Filtered two – fluid model

Filtered continuity and momentum conservation equations

10) $$\frac{\partial \left(\rho_s \bar{\phi}_s \right)}{\partial t} + \nabla . \left(\rho_s \bar{\phi}_s \tilde{\mathbf{v}}_s \right) = 0$$

11) $$\frac{\partial \left(\rho_g \bar{\phi}_g \right)}{\partial t} + \nabla . \left(\rho_g \bar{\phi}_g \tilde{\mathbf{v}}_g \right) = 0$$

12) $$\left[\frac{\partial \left(\rho_s \bar{\phi}_s \tilde{\mathbf{v}}_s \right)}{\partial t} + \nabla . \left(\rho_s \bar{\phi}_s \tilde{\mathbf{v}}_s \tilde{\mathbf{v}}_s \right) \right] = -\nabla . \bar{\boldsymbol{\sigma}}_s - \nabla . \boldsymbol{\tau}'_s - \bar{\phi}_s \nabla . \tilde{\boldsymbol{\sigma}}_g + \left(\mathbf{B}'_{gs} + \bar{\boldsymbol{M}}_I \right) + \rho_s \bar{\phi}_s \mathbf{g}$$

13) $$\left[\frac{\partial \left(\rho_g \bar{\phi}_g \tilde{\mathbf{v}}_g \right)}{\partial t} + \nabla . \left(\rho_g \bar{\phi}_g \tilde{\mathbf{v}}_g \tilde{\mathbf{v}}_g \right) \right] = -\bar{\phi}_g \nabla . \tilde{\boldsymbol{\sigma}}_g - \nabla . \boldsymbol{\tau}'_g - \left(\mathbf{B}'_{gs} + \bar{\boldsymbol{M}}_I \right) + \rho_g \bar{\phi}_g \mathbf{g}$$

Filtered volumetric continuity

14) $$\bar{\phi}_g + \bar{\phi}_s = 1$$

Closure for effective drag

Filtered drag force

15) $$\bar{\boldsymbol{M}}_I = \overline{\beta \left(\boldsymbol{v}_g - \boldsymbol{v}_s \right)}$$

Buoyancy fluctuation force (viscous terms are usually disregarded as lower order)

16) $$\boldsymbol{B}'_{gs} = -\left[\overline{\varphi_s \nabla \cdot \boldsymbol{\sigma}_g} - \bar{\varphi}_s \nabla \cdot \bar{\boldsymbol{\sigma}}_g \right] \approx -\left[\overline{\varphi_s \nabla P_g} - \bar{\varphi}_s \nabla \bar{P}_g \right]$$

Effective drag force

17) $$\beta_{eff} \left(\tilde{\boldsymbol{v}}_g - \tilde{\boldsymbol{v}}_s \right) = \boldsymbol{B}'_{gs} + \bar{\boldsymbol{M}}_I$$

18) $$\beta_{eff} = \frac{\overline{\beta \left(\boldsymbol{v}_g - \boldsymbol{v}_s \right)}}{\left(\tilde{\boldsymbol{v}}_g - \tilde{\boldsymbol{v}}_s \right)} - \frac{\left[\overline{\varphi_s \nabla P_g} - \bar{\varphi}_s \nabla \bar{P}_g \right]}{\left(\tilde{\boldsymbol{v}}_g - \tilde{\boldsymbol{v}}_s \right)}$$

The drag coefficient correction is defined as:

19) $$H = 1 - \frac{\beta_{eff}}{\bar{\beta}}$$

Further closures may be found in Mouallem et al. (2018).

2.3 Simulations and filtering

Highly resolved simulations were used for a typical fluid catalytic cracking particulate, with periodic boundary conditions. In all the simulations, particle diameter, particle density, gas density, and gas viscosity were set constant at 7.5×10^{-5} m, 1500 kg/m^3, 1.3 kg/m^3, 1.8×10^{-5} kg/(ms), respectively. Meantime, the free fall terminal velocity and the particle Froude number of the concerning particulate are 0.2184 m/s and 64.85, respectively. A two-dimensional square domain of 16 cm×16 cm was used with a numerical mesh of 128×128 grids. Several average axial gas flow rates were enforced over the domain, and statistical steady state conditions were achieved at various domain average gas Reynolds numbers. The domain average gas Reynolds number is defined as:

20) $$\left\langle \mathrm{Re}_g \right\rangle = \frac{\rho_g \mathrm{d}_p}{\mu_g} \left\langle \phi_g \right\rangle \left\langle \mathrm{v}_{g,y} \right\rangle$$

Domain average solid volume fractions $\langle \phi_s \rangle$ with aim of covering the dense regime of rapid riser flows were used 0.35, 0.45 and 0.50. Furthermore, the ratio between the domain average gas Reynolds number and its value under suspension conditions, $\left\langle \mathrm{Re}_g \right\rangle \Big/ \left\langle \mathrm{Re}_g \right\rangle_{susp}$, was set in a range covering flow conditions extending from fluidized suspensions up to topologies close to pneumatic transport (i.e. 1.0, 8.15, 16.30 and 24.45). $\left\langle \mathrm{Re}_g \right\rangle_{susp}$ results from imposing a gas pressure gradient in the axial direction over the domain that exactly matches the gravity acting on the gas-solid mixtures.

21) $$\Delta P_g = Y_{length} . g \left[\rho_s \left\langle \phi_s \right\rangle + \rho_g \left\langle \phi_g \right\rangle \right]$$

Where Y_{length} is the length of the domain in the axial direction. For obtaining filtered data from results of highly resolved simulations, a filtered square with the size of 2cm×2cm is defined to comprise a number of grids and made to sweep throughout the whole domain, collecting inside filter averages. In the filtering method, the collected averages are classified into bins by ranges of suitable independent variables (markers). In previous works the filtered solid volume fraction and the filtered slip velocity were identified as suitable markers for the effective drag coefficient (Milioli et al. 2013). In the current work, storage is done over 64×80 bins, meaning 64 gaps of solid volume fraction (1st marker) and 80 gaps of filtered slip velocity (2nd marker). All the simulations were done using MFIX, an open source code developed by NETL (National Energy Technology Laboratory, DOE-USA). The two-fluid model equations in MFIX are discretized through the finite volume method, and the resulting numerical code is solved through a point by point numerical technique. Comprehensive descriptions of MFIX modeling and numerical approaches can be found in this work (Syamlal et al. 1993, Syamlal 1998).

3. Results and discussion

Highly resolved simulations were performed for various cases of gas-solid fluidization under domain average solid volume fractions and domain average gas Reynolds numbers for evaluating the effects of those macro-scale parameters over the effective drag coefficient correction in the dense regime. Filtering procedure was performed inside the statistical steady state flow regime for the desired effective drag coefficient correction. Fig. 1 shows Snapshot of solid volume fraction over the whole domain for snapshots inside the statistical steady state regime. The pictures stand for simulations with domain average solid fractions (0.35, 0.45 and 0.50), and gas Reynolds number ratios 1. The figures show a considerable effect of this parameter over the flow topology. As can be seen, an increase on domain average solid volume fraction for a given gas Reynolds number ratio gives rise to denser and thicker structures. Additionally, it can be observed that with increase of solid volume fraction the flow will be more homogeneous.

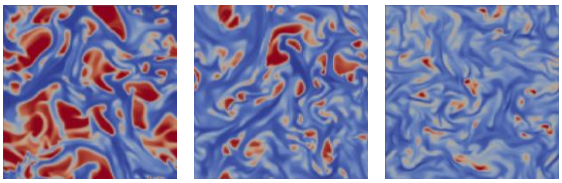

Figure 1. Snapshot of solid volume fraction for 0.35, 0.45 and 0.50 from left to right

Results for the drag coefficient correction (H), are presented in Fig. 2 and Fig. 3 as a function of the filtered solid volume fraction $\bar{\phi}_s$ and the dimensionless filtered axial slip velocity $\tilde{v}_{slip,y}/v_t$, for various dense domain average solid volume fraction $\langle \phi_s \rangle$ and gas Reynolds number ratios $\langle Re_g \rangle / \langle Re_g \rangle_{susp}$. The results are presented for a unique dimensionless filter size $\Delta_f/(v_t^2/g) = 4.112$, corresponding to a 2 cm×2 cm filtered square box. As can be seen in Fig. 2, a higher domain average gas Reynolds number causes H to decrease. Additionally, at lower domain average solid volume fraction, this effect becomes more prominent at lower filtered solid volume fractions and lower filtered slip velocities. This behavior comes from the flow becoming more homogeneous at higher solid fractions. However, this effect can be negligible with increase of average solid volume fraction. It is important to mention that, for more homogeneous situation of flow the amount of H is smaller. For instance, Fig. 2c proves that due to the more homogeneous situation has smaller H as comparison to other cases. Also Fig. 2 proves that at very high slip velocities and average solid volume fraction the effect of the gas Reynolds number ratio becomes not significant. For instance, at average solid volume fraction 0.50 (Fig. 2c), domain average gas Reynolds number has no effect. In this way, Fig. 3 shows more clearly the effects of the domain average solid volume fraction over H. As can be seen, $\langle \phi_s \rangle$ has little impact over H. however with increase of gas Reynolds number ratios, the effect of $\langle \phi_s \rangle$ becomes more significant. In general, Fig. 2 and Fig. 3 show that H is slightly affected by both the domain average gas Reynolds number and the domain average solid volume fraction in dense gas-solid flow.

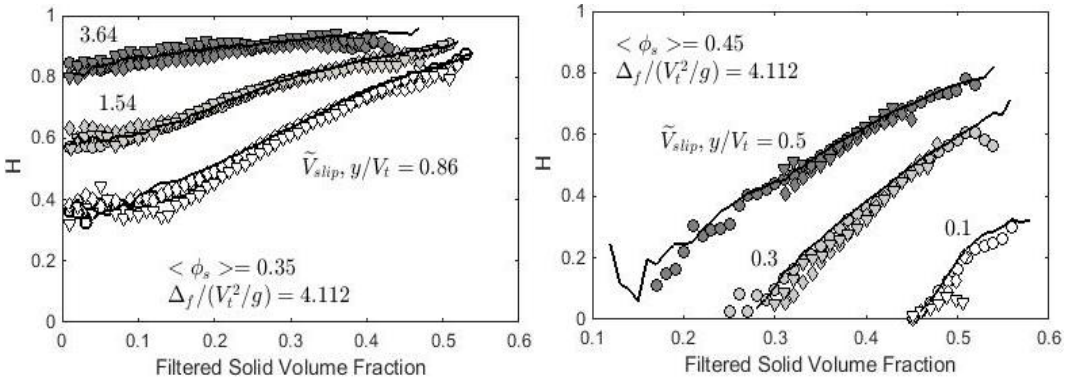

(a) (b)

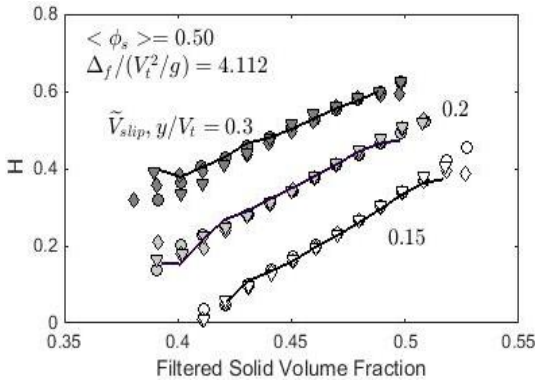

(c)

Figure 2. Drag coefficient correction, H, as a function of the filtered solid volume fraction and the dimensionless filtered axial slip velocity $\tilde{v}_{slip,y}/v_t$ for various domain average solid volume fraction and gas Reynolds number ratio, $\langle Re_g \rangle / \langle Re_g \rangle_{susp}$ = 1 (—), 8.15 (O), 16.30 (◊) and 24.45 (▼)

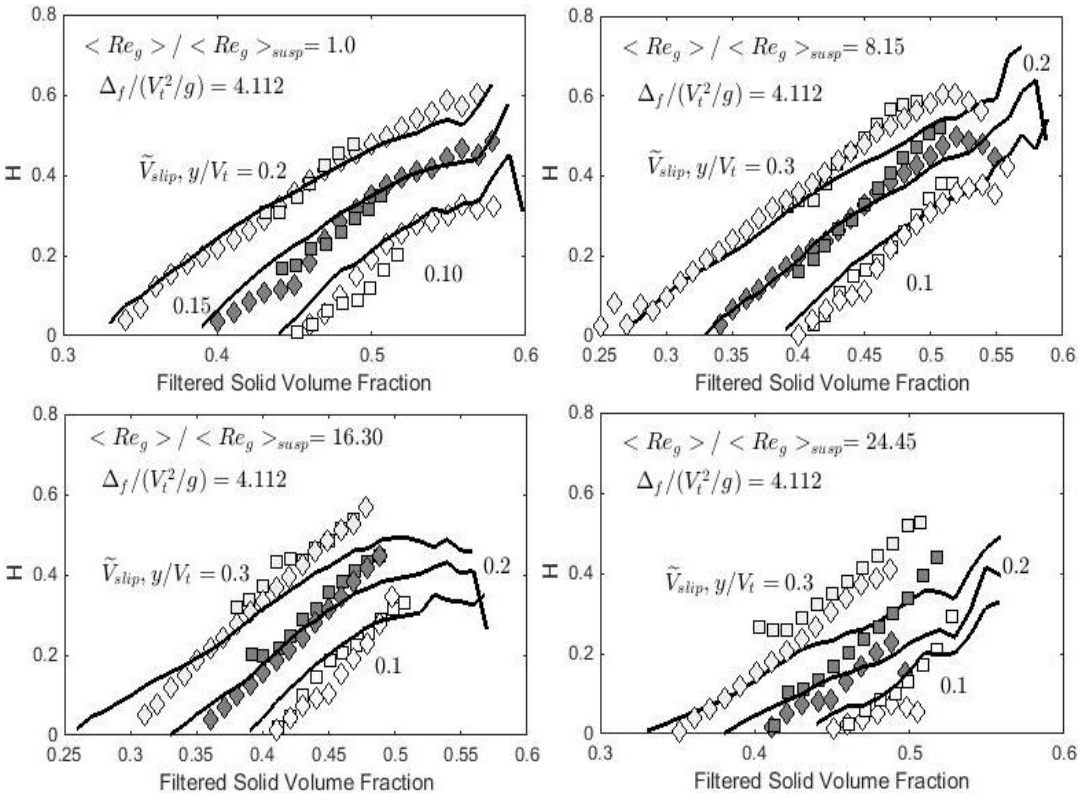

Figure 3. Drag coefficient correction, H, as a function of the filtered solid volume fraction and the dimensionless filtered axial slip velocity $\tilde{v}_{slip,y}/v_t$, for domain average solid volume fraction $\langle \phi_s \rangle$ = 0.35 (black lines), 0.45 (◊) and 0.50 (□), and for gas Reynolds number ratios $\langle Re_g \rangle / \langle Re_g \rangle_{susp}$ = 1, 8.15, 16.30 and 24.45

4. Conclusion

This article shows an evaluation of the effects of macro-scale parameters, domain average solid volume fraction and the domain average gas Reynolds number, associated to the flow topology on the effective drag in dense gas-solid riser flows. The analysis was performed using results of highly resolved simulations with microscopic two-fluid modeling. The simulations were carried out with the open source code MFIX on 2D periodical domains under average solid volume fractions (0.35, 0.45 and 0.50) and gas flow Reynolds numbers ratio (1, 8.15, 16.30 and 24.45). Additionally, in the next step, the simulations were filtered with snapshots taken inside the statistical steady state flow regime, applying space filters that were made to sweep all over the domain to collecting suitable statistics of relevant filtered parameters. Those filtered data were classified as a function of filtered solid volume fraction and the filtered slip velocity. Results reveal that in the dense regime due to the homogeneous behavior, the effective drag, expressed as a drag coefficient correction, is slightly affected by both the domain average solid volume fraction and the domain average gas Reynolds number.

5. Acknowledgements

This work was supported by The State of São Paulo Research Foundation (FAPESP), The National Council for Scientific and Technological Development (CNPq), and The Coordination for the Improvement of Higher Level Personnel (CAPES), all from Brazil.

Notation

$\boldsymbol{B}'$	fluctuation of gas-solid buoyancy force (Nm^{-3})
C_D	single particle drag coefficient (nd)
d_p	particle diameter (m)
$\boldsymbol{g}$, g	acceleration of gravity (ms^{-2})
H	drag coefficient correction (nd)
J_{coll}	rate of dissipation of granular energy by collisional damping ($Jm^{-3}s^{-1}$)
J_{vis}	rate of dissipation of granular energy by viscous damping ($Jm^{-3}s^{-1}$)
$\boldsymbol{M}$	drag force (Nm^{-3})
P	pressure (Nm^{-2})
Re_p	particle size based Reynolds number (nd)
t	time (s)
$\boldsymbol{v}$	velocity vector (ms^{-1})
y	vertical (axial) Cartesian coordinate (m)
	Greek Letters
β	micro-scale gas-solid drag coefficient (kgm-3s-1)
Γ_{slip}	rate of production of granular energy by gas-particle slip (Jm-3s-1)
Δ_f	filter size (m)
ε_p	particle sphericity (nd)
Θ	granular temperature (m2s-2)
κ_s	granular thermal conductivity (kgm-1s-1)
ρ	density (kgm-3)
$\boldsymbol{\sigma}$	deviatoric stress tensor (Nm-2)
$\boldsymbol{\tau}'$	Reynolds like stress tensor (Nm-2)
ϕ	volume fraction (nd)
	Subscripts
eff	effective, or meso-scale related
g	gas phase
I	interface
s	solid phase
$\overline{}$	filtered or volume average
~	Favre or mass weighed average, $\tilde{f} = \frac{\overline{\phi f}}{\overline{\phi}}$

6. References

Agrawal, Kapil, William Holloway, Christian C Milioli, Fernando E Milioli, and Sankaran Sundaresan. 2013. "Filtered models for scalar transport in gas–particle flows." *Chemical Engineering Science* 95:291-300.

Anderson, T Bo, and Roy Jackson. 1967. "Fluid mechanical description of fluidized beds. Equations of motion." *Industrial & Engineering Chemistry Fundamentals* 6 (4):527-539.

Andrews IV, Arthur T, Peter N Loezos, and Sankaran Sundaresan. 2005. "Coarse-grid simulation of gas-particle flows in vertical risers." *Industrial & engineering chemistry research* 44 (16):6022-6037.

Enwald, Hans, Eric Peirano, and A-E Almstedt. 1996. "Eulerian two-phase flow theory applied to fluidization." *International Journal of Multiphase Flow* 22:21-66.

Gidaspow, Dimitri. 1994. *Multiphase flow and fluidization: continuum and kinetic theory descriptions*: Academic press.

Igci, Yesim, and Sankaran Sundaresan. 2011. "Verification of filtered two-fluid models for gas-particle flows in risers." *AIChE Journal* 57 (10):2691-2707.

Lun, CKK, S Br Savage, DJ Jeffrey, and N Chepurniy. 1984. "Kinetic theories for granular flow: inelastic particles in Couette flow and slightly inelastic particles in a general flowfield." *Journal of fluid mechanics* 140:223-256.

Milioli, Christian C, Fernando E Milioli, William Holloway, Kapil Agrawal, and Sankaran Sundaresan. 2013. "Filtered two-fluid models of fluidized gas-particle flows: new constitutive relations." *AIChE Journal* 59 (9):3265-3275.

Mouallem, Joseph, Norman Chavez-Cussy, Seyed RA Niaki, Christian C Milioli, and Fernando E Milioli. 2018. "On the effects of the flow macro-scale over meso-scale filtered parameters in gas-solid riser flows." *Chemical Engineering Science*.

Niaki, S.R.A., Mouallem, J., Chavez-Cussy, N., Netzlaff, G.J.S., Milioli, C.C. and Milioli, F.E. 2017. "Effect of the flow Macro-Scale on the effective drag coefficient in Gas-Solid flows". *In Proceedings of the 24st International Congress of Mechanical Engineering - COBEM2017*, Curitiba, Brazil.

Ozel, A, Pascal Fede, and Olivier Simonin. 2013. "Development of filtered Euler–Euler two-phase model for circulating fluidised bed: high resolution simulation, formulation and a priori analyses." *International Journal of Multiphase Flow* 55:43-63.

Parmentier, Jean-François, Olivier Simonin, and Olivier Delsart. 2012. "A functional subgrid drift velocity model for filtered drag prediction in dense fluidized bed." *AIChE Journal* 58 (4):1084-1098.

Sarkar, Subir Kumar, Tiptur Gangaraju Basavaraju, and C Puttamadappa. 2016. *Ad hoc mobile wireless networks: principles, protocols, and applications*: CRC Press.

Schneiderbauer, Simon, and Stefan Pirker. 2014. "Filtered and heterogeneity-based subgrid modifications for gas–solid drag and solid stresses in bubbling fluidized beds." *AIChE Journal* 60 (3):839-854.

Syamlal, Madhava. 1998. MFIX documentation numerical technique. EG and G Technical Services of West Virginia, Inc., Morgantown, WV (United States).

Syamlal, Madhava, William Rogers, and Thomas J OBrien. 1993. MFIX documentation theory guide. USDOE Morgantown Energy Technology Center, WV (United States).

7. Responsibility Notice

The authors are the only responsible for the printed material included in this paper.